

# Comparison between three-dimensional CT and conventional radiography in proximal tibia morphology

Yijie Zhang, MD, Yanxi Chen, MD PhD\*, Minfei Qiang, MD, Kun Zhang, MD, Haobo Li, MD, Yuchen Jiang, MD, Xiaoyang Jia, MD

## Abstract

To provide morphological parameters of the normal tibial plateau by using three-dimensional (3D) CT and conventional radiography.

We performed morphological measurements of tibial plateau on 157 consecutive adults using radiographic and 3D computed tomography (CT). Gender differences as well as differences in measurement techniques were statistically compared. Intraclass correlation coefficient (ICC) was used to evaluate intra- and interobserver reproducibility.

The mediolateral dimensions, anteroposterior dimensions of tibial plateau showed significant differences according to gender, but no statistical differences were observed in coronal tibial slope as well as in posterior slope. There were significant differences in all parameters between 2 measurement techniques. 3D-CT measurements had a higher ICC in all parameters than that in the radiographs.

This study confirmed that 3D morphological measurements of tibial plateau have more reproducibility than radiographs. Our data will be helpful for tibial component design and placement.

**Abbreviations:** 2D-CT = two-dimensional computed tomography, 3D = three-dimensional, 3D-CT = three-dimensional computed tomography, AP = anteroposterior, CI = confidence interval, CT = computed tomography, CTS = coronal tibial slope, ICC = intraclass correlation coefficient, ML = mediolateral, OA = osteoarthritis, PS = posterior slope, SSD = surface shaded display, TAA = tibial anatomic axis, TKA = total knee arthroplasty.

**Keywords:** anthropometry, computed tomography, imaging, three-dimensional, tibia, tomography, x-ray computed

## 1. Introduction

Total knee arthroplasty (TKA) is widely used in the advanced stages of knee osteoarthritis, which could bring a pain-free knee to those who suffered. It is reported that rebuilding the native shape of the knee in TKA played an important role in clinical outcomes.<sup>[1,2]</sup> Morphometry of normal tibial plateau has been studied by many researchers.<sup>[3–8]</sup> They carried on measurements on plain radiographs and two-dimensional computed tomography (2D-CT) scan, and provided the basis for designing the tibial component. Recently, many disadvantages of measurements on plain radiographs and 2D-CT scan had been reported. Measurements on plain radiographs could be affected by foot rotation,<sup>[9]</sup> and medial and lateral tibial plateau are superimposed in lateral radiographs.<sup>[10–12]</sup> 2D-CT is more sensitive than radiography, but the selection of the observation plane for 2D-CT is still

influenced by the position of the knee and the reconstruction interval.<sup>[13–15]</sup> High intraclass correlation coefficients (ICC) were found in measurements on three-dimensional computed tomography (3D-CT),<sup>[16,17]</sup> which means 3D-CT could be used for a clear consensus of the measurements. However, to date, no study has reported whether there is a difference between radiographs and 3D-CT for measurement of normal tibial plateau.

The purposes of this study were to take anthropometric measurements of tibial plateau on 3D-CT; to assess difference in using radiographs and 3D-CT measuring methods; and to evaluate the reproducibility among the measurement techniques.

## 2. Methods

### 2.1. Subjects

From November 2013 to February 2015, 185 participants were retrospectively involved in the study. We exclude the participants with evidence of fracture, knee osteoarthritis (OA), or postoperative tibial plateau, which were confirmed by radiological examination. Finally, a total of 157 tibial plateau from 157 participants (87 males, 71 females; mean age: 47.5 years; range: 28–70 years) were included. Ethical approval was obtained from the Committee of the Medical Ethics of the hospital. All participants provided their written informed consent in this study.

### 2.2. Radiology technique and 3D bone models

The radiographs of the knee in non-weight-bearing position were obtained. CT scans were performed by a 32-detector CT scanner (GE Light-Speed CT; Waukesha, WI). The scanning protocol was

Editor: Heye Zhang.

The authors have no conflicts of interest to disclose.

Department of Orthopaedic Trauma, East Hospital, Tongji University School of Medicine, Shanghai, China.

\* Correspondence: Yanxi Chen, Shanghai East Hospital, Tongji University School of Medicine, Shanghai, China (e-mail: cyxtongji@126.com).

Copyright © 2018 the Author(s). Published by Wolters Kluwer Health, Inc. This is an open access article distributed under the terms of the Creative Commons Attribution-Non Commercial-No Derivatives License 4.0 (CCBY-NC-ND), where it is permissible to download and share the work provided it is properly cited. The work cannot be changed in any way or used commercially without permission from the journal.

Medicine (2018) 97:30(e11632)

Received: 1 April 2017 / Accepted: 30 June 2018

<http://dx.doi.org/10.1097/MD.0000000000011632>

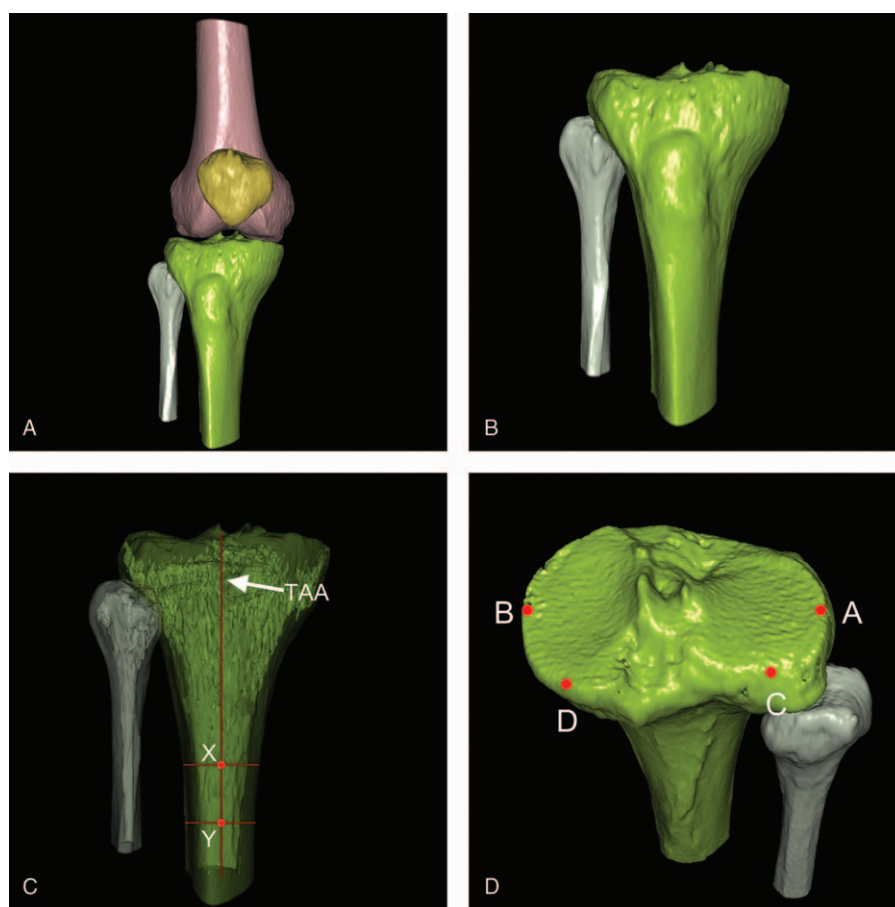


**Figure 1.** The process of generating the 3D structure of the tibial plateau and definition of point, line on it. (A) Tibial plateau and other bones of the knee were reconstructed into a 3D bone model by surface shaded display (SSD), and different colors were assigned to the different bones. (B) After hiding femur and patella, the tibial plateau was extracted solely. (C) Line XY= Tibial anatomic axis (TAA) in perspective mode. (D) A=the lateral most point of the tibial plateau, B=the medial most point of the tibial plateau, C=the posterior-most point of the lateral tibial condyle, D=the posterior-most point of the medial tibial condyle.

as follows: section thickness, 0.625 mm; tube voltage, 120 kVp; pitch, 1.375; matrix,  $512 \times 512$ . ALL data were saved as DICOM 3.0 format (.dcm), which then imported into a workstation (SuperImage orthopedics edition 1.1, Cybermed Ltd, Shanghai, China).<sup>[18]</sup> Then tibial plateau and other bones of the knee were reconstructed into a 3D bone model by surface shaded display (SSD), and different colors were assigned to the different bones (Fig. 1A). After hiding femur and patella, the tibial plateau was extracted solely (Fig. 1B).

### 2.3. Measuring procedures and parameters

The landmarks we used in measurements on radiographic and 3D-CT were previously described by Rasmussen<sup>[19]</sup> and Hashemi et al,<sup>[11]</sup> including: Tibial anatomic axis (TAA): TAA was determined by line passing through the 2 point (points X and Y), which were the midpoint of distal tibial shaft (Fig. 1C), the lateral most point of the tibial plateau (point A), the medial most point of the tibial plateau (point B), the posterior-most point of the lateral tibial condyle (point C), the posterior-most point of the medial tibial condyle (point D) (Fig. 1D).

After assessing and defining the above landmarks, 3D-CT measurement and radiographic measurement were as follows:

The mediolateral (ML) dimension: in the 3D-CT, it was the dimension of the line AB (Fig. 2A). In the radiographs, it was the

dimension of the line joining the peak point of the medial and lateral tibial plateau (Fig. 2D).

The anteroposterior (AP) dimension tibial plateau: in the 3D-CT, it was the dimension of the line AP, which was drawn perpendicular to the line ML and passed through the midpoint of it. MAP/LAP was the line drawn parallel to the line AP, which passed through point D/point C (Fig. 2A). In the radiographs, AP was the dimension of the line tangent to the articular surface of the plateau (Fig. 2D).

The coronal tibial slope (CTS): in the 3D-CT, it was the intersection of line AB and TAA (Fig. 2B). In the radiographs, it was measured by the intersection of the long axis of the tibial shaft and a line passing the peak lateral most and medial most point of the plateau (Fig. 2E).

The tibial plateau posterior slope (PS): in the 3D-CT, MTPS/lateral tibial posterior slope (LTPS) was the intersection of line MAP/LAP and TAA. The intersection of line MAM/LALBB and TAA (Fig. 2C). In the radiographs, PS was measured by the intersection of the long axis of the tibial shaft and a line tangent to the articular surface of the plateau (Fig. 2F).

### 2.4. Intraclass correlation coefficient

ICC was used to assess intra- and interobserver reliability of each measurement technique. 50 randomly selected subjects were

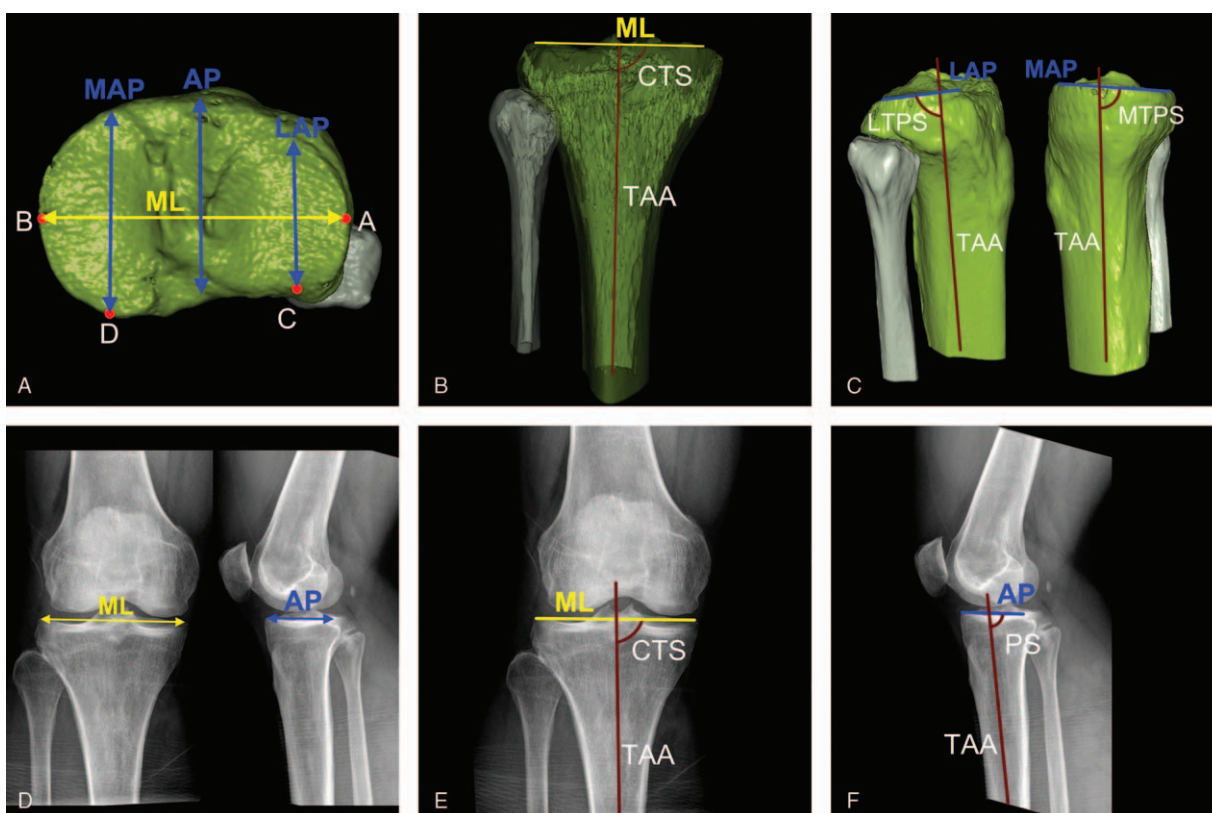


**Figure 2.** Morphological measurements of the tibial plateau. (A) ML dimension was taken as dimension of line AB. The AP was drawn perpendicular to the line ML and passed through the midpoint of it. MAP/LAP was the line drawn parallel to the line AP, which passed through point D/point C. (B) CTS was the intersection of ML and TAA. (C) MTSP/LTAP was the intersection of line MAP/LAP and TAA. (D) ML dimension was dimension of the line joining the peak point of the medial and lateral tibial plateau. (E) CTS was measured by the intersection of the long axis of the tibial shaft and a line passing the peak lateral most and medial most point of the plateau. (F) PS was measured by the intersection of the long axis of the tibial shaft and a line tangent to the articular surface of the plateau. 3D-CT=three-dimensional computed tomography, AP=anteroposterior dimension, CTS=coronal tibial slope, LAP=lateral anteroposterior dimension, MAP=media anteroposterior dimension, ML=mediolateral dimension, MTSP=medial tibial posterior slope, PS=posterior slope.

chosen to repeat the measurements by the main observer with 2-week interval to test the intraobserver reliability. The second observer repeated the measurements for 50 randomly selected knees to test the inter-observer reliability. The ICC was set at a desired lower limit of 0.8 and a 95% confidence interval (CI) of 0.2.

### 2.5. Statistical analysis

Statistical analysis was performed by using SPSS software 16.0 (SPSS, Chicago, IL). ICC was evaluated using the 2-way random effects model assuming a single measurement and absolute agreement. An ICC of 1 was characterized as perfect. The data were summarized as mean and standard deviation. The independent *t*-test was used to compare differences between genders. Paired *t*-test was used to determine the significance of differences in 2 measurement techniques. All differences were considered significant when  $P < .05$ .

### 3. Result

Table 1 summarized measurements of tibial plateau over all subjects and also within the 2 gender groups separately. The average ML, AP, MAP, and LAP in the male group were significantly greater than those in the female group ( $P < .05$  for each).

However, there was no significant gender difference in CTS, MTSP, and LTSP. ( $P > .05$  for each) (Table 1).

There were significant differences in all parameters between 3D-CT measurements and radiographic measurements ( $P < .05$ ) (Table 2).

In intra- and interobserver reliability of 3D-CT measurements, ICC values of every parameter were  $>0.8$ , which means excellent agreement. ICC value of 3D-CT measurement in every parameter was higher than that of radiographs (Fig. 3).

### 4. Discussion

TKA is considered as a precise surgical procedure to rebuild the native shape of the knee. Fully understanding about the morphometry of normal tibial plateau is helpful for the choice of implant's size, placement, and component design. Measurements based on 3D-CT had been proved more reproducible than plain radiography in many studies.<sup>[17,20,21]</sup> Qiang et al<sup>[21]</sup> revealed that when measuring distal tibiofibular syndesmosis, the reliability of 3D-CT measurement (ICC range, 0.907 to 0.972) was greater than radiographs (ICC range 0.742–0.838). Similar results were obtained in our study. The intra- and interobserver reproducibility of 3D-CT measurements in tibial plateau were more excellent.

ML and AP dimension were the commonly assessed parameters in TKA. A good match in ML and AP between

**Table 1**  
Anatomical parameters of tibial plateau.

	Mean $\pm$ SD			Sex difference	
	Total	Male	Female	t value	P value
3D-CT scans					
ML, mm	72.45 $\pm$ 5.29	75.90 $\pm$ 3.90	68.28 $\pm$ 3.39	-12.895	<.05*
AP, mm	42.37 $\pm$ 3.42	44.44 $\pm$ 2.75	39.86 $\pm$ 2.30	-11.155	<.05*
MAP, mm	44.50 $\pm$ 3.67	46.66 $\pm$ 2.69	41.88 $\pm$ 2.92	-10.294	<.05*
LAP, mm	40.33 $\pm$ 3.65	42.44 $\pm$ 3.07	37.78 $\pm$ 2.49	-10.663	<.05*
CTS (°)	3.26 $\pm$ 1.93	3.28 $\pm$ 1.95	3.23 $\pm$ 1.91	-0.171	.864
MTPS (°)	8.00 $\pm$ 2.94	8.24 $\pm$ 2.89	7.71 $\pm$ 2.99	-1.117	.266
LTPS (°)	5.62 $\pm$ 2.47	5.70 $\pm$ 2.41	5.52 $\pm$ 2.56	-0.466	.642
Radiographs					
ML, mm	75.49 $\pm$ 6.11	79.19 $\pm$ 4.92	71.01 $\pm$ 4.08	-11.188	<.05*
AP, mm	45.67 $\pm$ 4.28	48.01 $\pm$ 3.43	42.84 $\pm$ 3.43	-9.400	<.05*
CTS (°)	4.21 $\pm$ 2.32	4.31 $\pm$ 2.29	4.09 $\pm$ 2.35	-0.608	.544
PS (°)	8.33 $\pm$ 2.78	8.57 $\pm$ 2.54	8.03 $\pm$ 3.03	-0.755	.451

3D-CT = three-dimensional computed tomography, AP = anteroposterior dimension, CTS = coronal tibial slope, LAP = lateral anteroposterior dimension, LTPS = lateral tibial posterior slope, MAP = medial anteroposterior dimension, ML = mediolateral dimension, MTPS = medial tibial posterior slope, PS = posterior slope, SD = standard deviation.

\* Statistically significant ( $P < .05$ ).

**Table 2**  
Comparison of parameters in different image modalities.

	t value	P value
3D-CT/radiographic		
ML	-4.025	<.05*
AP	-6.491	<.05*
CTS	-4.097	<.05*

3D-CT = three-dimensional computed tomography, AP = anteroposterior dimension, CTS = coronal tibial slope, ML = mediolateral dimension.

\* Statistically significant ( $P < .05$ ).

tibial component and resected tibial surface would lead to good stress distribution and stability, which was a key factor for long-term good results.<sup>[22,23]</sup> Yang et al<sup>[6]</sup> revealed that MAP dimension was larger than LAP dimension, which were consistent with the findings of this study. Although the potential advantages of asymmetric tibial component were reported by many researchers<sup>[22,24]</sup>, manufacturers paid less attention to it and still offered symmetric tibial components. As symmetric components are still used clinically, discrepancy between MAP and LAP dimensions would result in mismatch. For a given ML dimension, if LAP dimension of component was perfectly fit for the tibial, the component would undersize in MAP direction. Subsidence was more common to see with an undersized component.<sup>[25]</sup> However, if MAP dimension of component was chosen to fit the tibia, the component would overhang in LAP direction. An overhanging component would result in soft tissue irritation and pain.<sup>[2,26]</sup> Therefore, a well-matched component would avoid aforementioned complications.

Coronal tibial slope was reported as a determining factor during operation to predict the postoperative standing femorotibial angle.<sup>[27]</sup> Hashemi et al<sup>[11]</sup> measured normal tibia and revealed that coronal tibial slopes 98% of the subjects were positive or zero. In the present study, we had similar findings, which means that in a majority of subjects the lateral tibial plateau has a superior edge than the medial. The original coronal tibial slope of the patient would be reproduced during TKA if surgeon placed the tibial component at the specific slope. Furthermore, understanding coronal tibial slope differences among subjects could help design a more accurate implant that restore the biomechanics of the normal knee.

The tibial plateau posterior slope is considered important in anteroposterior stability and knee kinematics.<sup>[28,29]</sup> Furthermore, published literature reported an increased PTS could lead to an increased incidence of anterior cruciate ligament rupture.<sup>[30]</sup> A 3° to 7° PTS in the proximal tibial osteotomy is recommended in TKA. Tsukeoka et al<sup>[31]</sup> found a large PTS such as 7° or 10° might contribute to a tremendous change in the alignment of the tibia in TKA. An excessive posterior slope when cutting the tibia would lead to flexion instability while a smaller or even anterior slope would cause decreased knee flexion.<sup>[28,32]</sup>

It is known that the radiation exposure of CT is higher compared to that of conventional radiography. However, in our opinion, the improved accuracy may justify the added radiation dose. A postoperative CT is considered the standard for assessment of reduction.<sup>[33]</sup> According to our data, 3D-CT could improve measurement accuracy. Besides, several techniques,<sup>[34]</sup> protocol modifications,<sup>[35]</sup> the latest generation of CT machines could markedly lower radiation doses.<sup>[36–38]</sup>

Other imaging modalities such as ultrasound or MR imaging could also serve as an important tool to assess the anatomy and the injuries of the knee. Ultrasound is a reliable noninvasive method to assess the pathologic condition of the knee joint, such as injuries of the tendons, ligaments and muscles, osteoarthritis, and osteochondral defects.<sup>[39]</sup> MR imaging has the advantage in demonstrating the extent and nature of fractures and assessing the soft tissue injury such as meniscal and anterior cruciate ligament tears.<sup>[40,41]</sup>

The present study had several limitations. First, our study was lack of comparison with measurements from cadavers. Therefore, value differences between 2 measurement techniques and cadaver measurements were not clear. Second, subjects in this study were healthy, rather than those with arthritic knees. Although the osteoarthritic knee had been deformed and had different dimensions from normal knee, our aim was to offer a clinical reference to help surgeon to rebuild the normal shape for those deformed knees.

## 5. Conclusions

This study confirmed that 3D morphological measurements of tibial plateau have more reproducibility than radiographs. In this population, males have a large ML, AP, MAP, and LAP



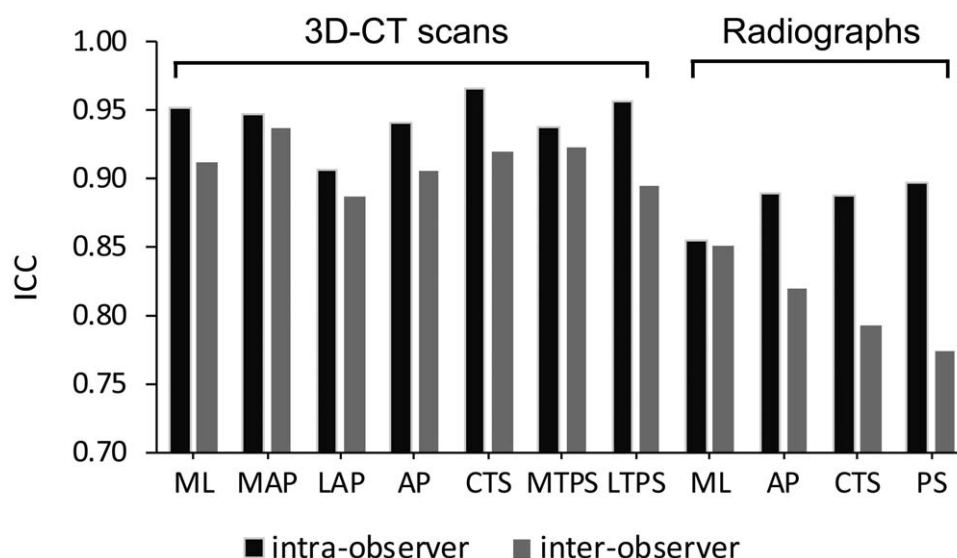


**Figure 3.** Intra- and interobserver reproducibility of 3D-CT and radiographic measurements.

dimensions than females, but there is no significant difference in CTS, MTPS, and LTPS between genders. Our data will be helpful for tibial component design and placement.

### Author contributions

**Conceptualization:** Yijie Zhang, Yanxi Chen.

**Data curation:** Yijie Zhang, Kun Zhang, Haobo Li, Yuchen Jiang, Xiaoyang Jia.

**Software:** Yijie Zhang.

**Supervision:** Yanxi Chen.

**Writing – original draft:** Yijie Zhang, Yanxi Chen, Minfei Qiang.

**Writing – review & editing:** Yijie Zhang, Yanxi Chen.

### References

- [1] Lee DH, Park JH, Song DI, et al. Accuracy of soft tissue balancing in TKA: comparison between navigation-assisted gap balancing and conventional measured resection. *Knee Surg Sports Traumatol Arthrosc* 2010;18:381–7.
- [2] Bonnin MP, Schmidt A, Basigliani L, et al. Mediolateral oversizing influences pain, function, and flexion after TKA. *Knee Surg Sports Traumatol Arthrosc* 2013;21:2314–24.
- [3] Erkokak OF, Kucukdurmaz F, Sayar S, et al. Anthropometric measurements of tibial plateau and correlation with the current tibial implants. *Knee Surg Sports Traumatol Arthrosc* 2016;24:2990–7.
- [4] Hitt K, Shurman JN, Greene K, et al. Anthropometric measurements of the human knee: correlation to the sizing of current knee arthroplasty systems. *J Bone Joint Surg Am* 2003;85-A(suppl 4):115–22.
- [5] Hafez MA, Sheikhedrees SM, Saweeris ES. Anthropometry of Arabian arthritic knees: comparison to other ethnic groups and implant dimensions. *J Arthroplasty* 2016;31:1109–16.
- [6] Yang B, Song CH, Yu JK, et al. Intraoperative anthropometric measurements of tibial morphology: comparisons with the dimensions of current tibial implants. *Knee Surg Sports Traumatol Arthrosc* 2014;22:2924–30.
- [7] Dai Y, Bischoff JE. Comprehensive assessment of tibial plateau morphology in total knee arthroplasty: Influence of shape and size on anthropometric variability. *J Orthop Res* 2013;31:1643–52.
- [8] Yue B, Varadarajan KM, Ai S, et al. Differences of knee anthropometry between Chinese and white men and women. *J Arthroplasty* 2011;26:124–30.
- [9] Lee YS, Lee BK, Lee SH, et al. Effect of foot rotation on the mechanical axis and correlation between knee and whole leg radiographs. *Knee Surg Sports Traumatol Arthrosc* 2013;21:2542–7.
- [10] Chiu KY, Zhang SD, Zhang GH. Posterior slope of tibial plateau in Chinese. *J Arthroplasty* 2000;15:224–7.
- [11] Hashemi J, Chandrashekar N, Gill B, et al. The geometry of the tibial plateau and its influence on the biomechanics of the tibiofemoral joint. *J Bone Joint Surg Am* 2008;90:2724–34.
- [12] Faschingbauer M, Sgroi M, Juchems M, et al. Can the tibial slope be measured on lateral knee radiographs? *Knee Surg Sports Traumatol Arthrosc* 2014;22:3163–7.
- [13] Wang T, Nakamoto K, Zhang H, et al. Reweighted anisotropic total variation minimization for limited-angle CT reconstruction. *IEEE Transact Nucl Sci* 2017;64:2742–60.
- [14] Huang Y, Taubmann O, Huang X, et al. Scale-space anisotropic total variation for limited angle tomography. *IEEE Trans Radiat Plasma Med Sci* 2018;2:1–1.
- [15] Gao Z, Liu X, Qi S, et al. Automatic segmentation of coronary tree in CT angiography images. *Int J Adapt Control* 2017;0:00–10.
- [16] Stirling E, Jeffery J, Johnson N, et al. Are radiographic measurements of the displacement of a distal radial fracture reliable and reproducible? *Bone Joint J* 2016;98-B:1069–73.
- [17] Weber M, Lechler P, von Kunow F, et al. The validity of a novel radiological method for measuring femoral stem version on anteroposterior radiographs of the hip after total hip arthroplasty. *Bone Joint J* 2015;97-B:306–11.
- [18] Chen YX, Zhang K, Hao YN, et al. Research status and application prospects of digital technology in orthopaedics. *Orthop Surg* 2012;4:131–8.
- [19] Rasmussen PS. Tibial condylar fractures. Impairment of knee joint stability as an indication for surgical treatment. *J Bone Joint Surg Am* 1973;55:1331–50.
- [20] Lee YK, Kim TY, Ha YC, et al. Radiological measurement of femoral stem version using a modified Budin method. *Bone Joint J* 2013;95-B:877–80.
- [21] Chen Y, Qiang M, Zhang K, et al. A reliable radiographic measurement for evaluation of normal distal tibiofibular syndesmosis: a multi-detector computed tomography study in adults. *J Foot Ankle Res* 2015;8:32.
- [22] Bonnin MP, Saffarini M, Shepherd D, et al. Oversizing the tibial component in TKAs: incidence, consequences and risk factors. *Knee Surg Sports Traumatol Arthrosc* 2016;24:2532–40.
- [23] Servien E, Saffarini M, Lustig S, et al. Lateral versus medial tibial plateau: morphometric analysis and adaptability with current tibial component design. *Knee Surg Sports Traumatol Arthrosc* 2008;16:1141–5.
- [24] Westrich GH, Haas SB, Insall JN, et al. Resection specimen analysis of proximal tibial anatomy based on 100 total knee arthroplasty specimens. *J Arthroplasty* 1995;10:47–51.

- [25] Chau R, Gulati A, Pandit H, et al. Tibial component overhang following unicompartmental knee replacement—does it matter? *Knee* 2009;16:310–3.
- [26] Mahoney OM, Kinsey T. Overhang of the femoral component in total knee arthroplasty: risk factors and clinical consequences. *J Bone Joint Surg Am* 2010;92:1115–21.
- [27] Terauchi M, Shirakura K, Kobuna Y, et al. Axial parameters affecting lower limb alignment after high tibial osteotomy. *Clin Orthop Relat Res* 1995;317:141–9.
- [28] Hudek R, Schmutz S, Regenfelder F, et al. Novel measurement technique of the tibial slope on conventional MRI. *Clin Orthop Relat Res* 2009;467:2066–72.
- [29] Stulberg SD. How accurate is current TKR instrumentation? *Clin Orthop Relat R* 2003;416:177–84.
- [30] Hashemi J, Chandrashekar N, Mansouri H, et al. Shallow medial tibial plateau and steep medial and lateral tibial slopes: new risk factors for anterior cruciate ligament injuries. *Am J Sports Med* 2010;38:54–62.
- [31] Tsukeoka T, Tsuneizumi Y, Lee TH. The effect of the posterior slope of the tibial plateau osteotomy with a rotational error on tibial component malalignment in total knee replacement. *Bone Joint J* 2013;95-B:1201–3.
- [32] Hofmann AA, Bachus KN, Wyatt RW. Effect of the tibial cut on subsidence following total knee arthroplasty. *Clin Orthop Relat Res* 1991;63–9.
- [33] Gosling T, Klingler K, Geerling J, et al. Improved intra-operative reduction control using a three-dimensional mobile image intensifier—a proximal tibia cadaver study. *Knee* 2009;16:58–63.
- [34] Feng C, Zhu D, Zou X, et al. The combination of a reduction in contrast agent dose with low tube voltage and an adaptive statistical iterative reconstruction algorithm in CT enterography: effects on image quality and radiation dose. *Medicine (Baltimore)* 2018;97:e151.
- [35] Razek AAKA, Tawfik AM, Elsorogy LGA, et al. Perfusion CT of head and neck cancer. *Eur J Radiol* 2014;83:537–44.
- [36] Paul J, Schell B, Kerl JM, et al. Effect of contrast material on image noise and radiation dose in adult chest computed tomography using automatic exposure control: a comparative study between 16-, 64- and 128-slice CT. *Eur J Radiol* 2011;79:e128–32.
- [37] Guberina N, Forsting M, Ringelstein A, et al. Radiation exposure during CT-guided biopsies: recent CT machines provide markedly lower doses. *Eur Radiol* 2018;doi: 10.1007/s00330-018-5350-1. [Epub ahead of print].
- [38] Fang R, Zhang S, Chen T, et al. Robust low-dose CT perfusion deconvolution via tensor total-variation regularization. *IEEE Trans Med Imaging* 2015;34:1533–48.
- [39] Razek AAKA, Fouda NS, Elmetwaley N, et al. Sonography of the knee joint. *J Ultrasound* 2009;12:53–60.
- [40] Skinner S. MRI of the knee. *Aust Fam Physician* 2012;41:867–9.
- [41] Mansour R, Kausik M, McNally E. MRI of knee joint injury. *Semin Musculoskelet Radiol* 2006;10:328–44.